International Journal of Geo-Information

Article

Rule-Based Scenario Classification Using Vehicle Trajectories

Sungmo Ku [1] and Jinho Lee [2,*]

1 Department of Smart Factory Engineering, Tech University of Korea, Siheung 15073, Gyeonggi-do, Republic of Korea; tndah06084@tukorea.ac.kr
2 Department of Computer Engineering, Tech University of Korea, Siheung 15073, Gyeonggi-do, Republic of Korea
* Correspondence: jhjy2491@tukorea.ac.kr

Abstract

Ensuring the safety of autonomous driving systems (ADS) requires scenario-based testing that reflects the complexity and variability of real-world driving conditions. However, the nondeterministic nature of actual traffic environments makes physical testing costly and limited in scope, particularly for rare and safety-critical scenarios. To address this, simulation has become a core component in validation by providing scalable, controllable, and repeatable testing environments. This study proposes a trajectory-based scenario classification framework that emphasizes both generality and interpretability. Specifically, we define a set of rule-based maneuver classification criteria using lateral acceleration patterns and apply them to simulated urban driving scenarios modeled with OpenSCENARIO. To address overlapping maneuver characteristics, a priority ordering of classification rules is introduced to resolve ambiguities. The proposed method was evaluated on a dataset comprising 7 types of maneuvers, including straight driving, lane changes, turns, roundabouts, and U-turns. Experimental results demonstrate the effectiveness of rule-driven classification based on vehicle trajectory dynamics and highlight the potential of this approach for structured scenario definition and validation in ADS simulation environments.

Keywords: driving trajectory classification; rule-based scenario classification; scenario generation; autonomous driving test; ISO 26262; ISO 21448 (SOTIF); OpenSCENARIO

Academic Editors: Wolfgang Kainz, Chaowei Yang, Daniel Q. Duffy, Xiao Huang and Lingbo Liu

Received: 3 December 2025
Revised: 1 January 2026
Accepted: 9 January 2026
Published: 11 January 2026

1. Introduction

The safety validation of Autonomous Driving Systems (ADS) faces fundamental challenges due to the inherent complexity, non-determinism, and unpredictability of real-world driving environments [1–3]. In particular, edge-case scenarios (i.e., rare but potentially safety-critical situations) are extremely difficult to reproduce and test repeatedly in physical environments. To address these limitations, simulation has emerged as a critical tool in the development and validation of autonomous vehicles, providing a controlled, repeatable, and scalable testing environment that can effectively complement the complexity of real-world driving conditions [4]. Simulation enables efficient reproduction and analysis of diverse driving scenarios, thereby facilitating early identification and mitigation of potential risks before the installation of the system on public roads.

To institutionalize simulation-based validation, several international standards have been established. These include ISO 26262 for functional safety, ISO 21448 (SOTIF) for the safety of intended functionality, and ASAM OpenX standards (i.e., OpenSCENARIO (https://www.asam.net/standards/detail/openscenario/ (accessed on 1 January 2026)) and OpenDRIVE (https://www.asam.net/standards/detail/opendrive/ (accessed on

1 January 2026)) for the structured definition of scenario components [5,6]. These standards clearly specify the static and dynamic elements of driving scenarios, supporting systematic verification of the behavior of ADS under various conditions.

In practice, real-world driving environments exhibit virtually infinite spatiotemporal variability. To effectively address this in simulations, a structured and scalable method for scenario classification and organization is essential. A representative approach in previous research is the layered classification framework proposed by the PEGASUS (https://www.pegasusprojekt.de/en/home (accessed on 1 January 2026)) project, which categorizes scenarios by Road Environment, Traffic Participants, and Additional Condition [7]. Alternatively, other studies classify scenarios based on vehicle dynamic states (i.e., vehicle state maneuver, infrastructure maneuver, and object-related maneuver) [8,9]. Although these hierarchical frameworks offer a structured view, they often fail to capture the diversity and generalizability of real-world driving conditions. Other approaches include ontology-based methods that define inter-object relationships at the scene level, as well as data-driven methods that utilize statistical analysis or deep learning models trained on real-world trajectories [10]. However, these methods also exhibit limitations in fully reflecting the richness and extensibility of real-world scenarios. Therefore, this study proposes a trajectory-centric framework for defining and classifying driving scenarios, aiming to balance generality and interpretability in vehicle behavior modeling. This approach seeks to establish a practical classification system grounded in trajectory data, and to construct reproducible units of scenarios that are suitable for simulation-based verification.

The necessity for such a trajectory-centric system is further highlighted by the ongoing efforts to bridge the gap between real-world data and virtual validation. While numerous studies have leveraged real-world driving data to reconstruct scenarios in standardized formats like OpenSCENARIO [11–15], their focus has primarily remained on the reproduction of individual events. For instance, research has identified ego-vehicle activities such as lane changes based on lane-boundary distances [11] or utilized specialized datasets like HighD to generate concrete scenarios for Automated Lane Keeping Systems [12,15]. However, these existing works often treat scenario generation as an isolated process, lacking a generalized framework that systematically integrates these scenarios across the broader learning and validation pipelines. Consequently, there remains a critical need for a methodology that not only generates scenarios but also organizes them into branching logical structures that enhance the scalability of autonomous driving algorithms. To address this gap, this study proposes a framework based on scenario branching to improve both the verifiability and the systematic utility of generated maneuvers.

The remainder of this paper is organized to systematically present the development and validation of the proposed trajectory-centric classification framework. In Section 2, we review related research across four key areas: safety testing for autonomous driving, vehicle behavior classification, scenario classification and indexing, and scenario generation. Section 3 introduces the proposed method, including the design and construction of the dataset, its key characteristics, and the classification strategy adopted by the model. The methodology section further details the rule-based classification process and the criteria used for maneuver discrimination. Additionally, the data analysis and rule formulation subsections describe the specific parameters and logic applied within the classification framework. In Section 4, we present the experimental results obtained from the proposed rule-based model, highlighting the necessity of rule prioritization and the outcomes of its application. This section also introduces parameter optimization as a technical means to mitigate initial classification errors and includes a comparative analysis with deep learning models to rigorously validate the performance and efficiency of the proposed framework. Section 5 provides a comprehensive discussion that critically examines the structural limitations of the current framework, the impact of dataset characteristics, and the challenges of cross-platform consistency across different simulators. Finally, Section 6 concludes the paper by summarizing the key contributions and outlining future research directions.

2. Related Work

Validation methods for ensuring the safety of autonomous driving systems are rapidly shifting from traditional function-level testing toward scenario-based testing frameworks. This approach aims to comprehensively cover the complex and diverse driving situations that autonomous vehicles can encounter, while improving the reproducibility and coverage of test cases in a meaningful way. To this end, it is necessary to understand both the validation of autonomous driving algorithms using scenarios and the processes of scenario generation and classification.

2.1. Scenario-Based Driving Safety Test

Recent autonomous driving test frameworks have increasingly adopted simulation-based components defined in alignment with international standards such as ISO 26262. From this perspective, the driving environment is no longer treated merely as a collection of visual elements, but is systematically decomposed into scenes, which represent static snapshots; situations, which capture decision-relevant contexts; and scenarios, which describe the temporal evolution of events [16].

Such formalized definitions provide a structural foundation for enhancing the reliability of simulation-based testing. To support this paradigm, research efforts have focused on extracting vehicle motions and behaviors from real-world physical data and converting the extracted information into standardized data formats such as OpenSCENARIO. Studies in [17,18] facilitate the generation of standardized datasets for autonomous driving tests using real-world data, while [19] extracts vehicle maneuvers and directly infers metadata at the scenario level, thereby reducing reliance on domain experts and enabling automated generation of repetitive test cases. Collectively, these studies contribute to the creation of realistic scenario representations for autonomous driving algorithm testing and reflect a broader transition toward data-driven or hybrid approaches for dynamic scenario construction. Such methods allow simulation-based testing environments to more effectively capture the variability and realism of real-world driving conditions, while supporting coverage-driven safety assessment.

2.2. Driving Maneuver Classification

Accurate classification of vehicle maneuvers during driving is a key factor in ensuring the safety of autonomous driving systems and enabling automation in scenario-based validation. Maneuver recognition and behavior classification techniques have evolved from early simple rule-based methods toward hybrid and deep-learning-based models designed to address the increasing complexity of urban driving environments.

Early studies focused on rule-based approaches to achieve high interpretability and real-time performance. In structured environments such as highways, it has been demonstrated that lane-change intentions and driving behaviors can be predicted with high accuracy using logical rules based on physical indicators such as lateral velocity, lane position, and time-to-collision (TTC) [20,21]. These approaches are characterized by low computational complexity, making them well suited for real-time implementation in Advanced Driver Assistance Systems (ADAS). However, rule-based approaches have difficulty capturing the complexity of urban environments. To address this limitation, Haque et al. [21] introduced a hybrid approach that combines refined rules with machine learning techniques. By detecting motion transitions from time-series sensor data and linking them with various classification models, such as Random Forest, Support Vector Machine (SVM), and Long Short-Term Memory (LSTM), the scope of maneuver classification was expanded [21–26]. Another line of research adopts deep-learning-based approaches that leverage large-scale driving data and probabilistic models. By integrating Hidden Markov Models (HMMs) with Variational Gaussian Mixture Models (VGMMs), these methods simultaneously predict surrounding vehicles' maneuvers and future trajectories, achieving significant performance improvements over simple motion models [27–29]. More recently, studies have combined domain knowledge and scenario information with transfer learning and attention mechanisms to maximize recognition accuracy in environments with low data density or high complexity, such as intersections and merging areas [30]. In addition, approaches that integrate models with heterogeneous characteristics through dual architectures or fuzzy logic have contributed to reducing classification errors in ambiguous driving situations and improving overall reliability [31–33].

Overall, driving maneuver classification techniques have progressed beyond simple event detection to form structured frameworks that account for diverse driving environments and sensor characteristics. This technological foundation plays a central role in scenario-based autonomous driving validation systems by supporting situation awareness and object behavior analysis.

2.3. Scenario Classification and Indexing

To quantitatively validate the reliability of autonomous driving systems, it is essential to move beyond raw log data and adopt a framework capable of systematically classifying and indexing complex driving environments. Recent studies have focused on semantically structuring large-scale driving data and developing logical modeling approaches for efficient extraction, storage, and generation of scenarios.

Considerable research has been devoted to semantic structuring methods that derive meaningful test units from real-world driving data. Representative approaches hierarchically organize vehicle maneuvers based on the relationships among vehicle states, road infrastructure, and surrounding objects, and parameterize these maneuvers to transform unstructured driving logs into interpretable scenario units [9,34]. Such methods provide a foundation for generalizing complex real-world driving behaviors into structured and reusable test cases. Database indexing and ontology-based techniques are equally important for systematically managing and reusing extracted scenarios. By decomposing scenarios into atomic components and storing them in object-centered, normalized data structures, environments have been established in which thousands of scenarios can be queried and managed using SQL-based operations [7,35]. In particular, knowledge-based ontology approaches enforce the generation of only valid combinations of road structures and traffic objects, thereby improving the consistency of scenario specifications and compensating for the expressive limitations of standard formats such as OpenSCENARIO [10]. More recently, increasing attention has been paid to analyzing logical relationships among scenarios in order to ensure validation completeness, or coverage. By defining scenario attributes using temporal logic languages (e.g., CMFTBL) and organizing them within tree-based classifiers, methods have been proposed to automatically identify scenario types contained in driving logs [36–38]. These approaches go beyond simple classification by enabling the detection of missing attribute combinations, thereby allowing quantitative evaluation of test coverage.

Comprehensively, scenario classification and indexing technologies have evolved from basic data storage mechanisms into intelligent management frameworks that integrate temporal logic with knowledge-based rules. Such frameworks serve as core infrastructure for ensuring reproducibility and efficiency in scenario-based validation processes for autonomous driving systems.

2.4. Scenario Generation

To maximize the efficiency of autonomous driving system validation, recent studies have leveraged international standards such as OpenSCENARIO not merely as specification tools but as central components of automated test generation frameworks. In particular, technical efforts have continued to move away from fixed-parameter-based, discrete testing approaches toward dynamically exploring and controlling a broad scenario space.

To enhance scenario flexibility, the constituent elements of a scenario—such as object placement, execution order, and decision-making logic—have been represented using hierarchical behavior trees, enabling more complex and variable scenario execution control within simulation environments [39]. This structured approach, when combined with automated generation pipelines, provides an environment in which a large number of test cases can be rapidly generated and executed in high-fidelity simulators such as CARLA. In addition, various hazardous situations can be tested by injecting disturbances such as risky vehicle cut-in maneuvers, pedestrian crossings, and adverse weather conditions into baseline scenarios [40]. By coupling these mechanisms with parameter space exploration guided by the Operational Design Domain (ODD), both scenario diversity and realism can be simultaneously achieved [41,42]. While scenario extraction from real-world data focuses on faithfully describing observed driving behavior, research on scenario generation places emphasis on testing a wide range of environments beyond those present in real datasets. This enables evaluation of system performance limits beyond simple functional verification.

As a result, recent studies utilizing the OpenSCENARIO standard have advanced the level of automation in scenario-based validation by integrating structured scenario definitions, parameter space exploration, and flexible execution control logic. This practical foundation provides the scalability required to quantitatively and systematically cover the vast range of driving situations that autonomous vehicles may encounter.

2.5. Contributions of the Proposed Framework

Existing studies on behavior classification and scenario indexing have primarily focused on partial driving behaviors occurring within limited spatial contexts, such as intersections or highways. In contrast, this study aims to distinguish generalized driving behaviors in expanded urban environments. Accordingly, the main contributions of this work to the field of scenario-based autonomous driving validation are as follows:

1. Trajectory-centric scenario classification framework: This study proposes a rule-based maneuver classification method that leverages lateral acceleration patterns to distinguish driving behaviors across a total of 7 major scenario types, comprising a fine-grained set of specific maneuvers. Unlike previous studies, which primarily focused on limited driving behaviors at crossroads and on highways, the proposed framework presents a high-level categorization of vehicle behaviors that can occur in urban environments. While learning-based models often function as black boxes, the proposed approach ensures transparency through a framework based on physical driving dynamics.
2. Simulation dataset construction based on OpenSCENARIO: A comprehensive simulation dataset was constructed based on OpenSCENARIO v1.2, encompassing seven trajectory-based urban driving scenarios under conditions without the influence of other vehicles. The dataset includes a variety of maneuver types, and driving speeds, and was designed with repeatability, coverage analysis, and future autonomous driving system testing.

3. Modeling generalized urban driving trajectories: In prior studies analyzing urban driving maneuvers and driver behavior, the focus has primarily been on straight driving, left turns, and right turns, with straight driving typically limited to linear road segments. In contrast, the present study considers a broader range of driving conditions by including straight driving on various curve roads as well as analyzing trajectories associated with roundabout maneuvers, thereby reflecting more generalized urban driving scenarios.
4. Quantitative analysis and performance evaluation of the rule-based classifier: In this study, classification rules were defined for each driving trajectory, and comparative experiments were conducted by varying the rule application order. This allowed us to identify which trajectories required more fine-grained conditions or additional classification criteria. Through this analysis, we provide insights into the prioritization and complexity of trajectory classification. The proposed rule-based classifier achieved high performance with an accuracy of 0.9784, an F1-score of 0.9764, and a processing speed of 74.42 samples per second. Furthermore, class-wise recall analysis revealed the strengths and limitations of the model.

3. Proposed Method

This section outlines the data acquisition process, key data characteristics, and the methodology used for maneuver classification. The dataset consists of two primary components: scenario files and driving log data. The scenario files define the entities, trajectories, and events to be simulated, while the driving logs capture the actual behavior of the vehicle as it executes each scenario within the simulator. This study proposes a classification approach based on the collected trajectory data. The following subsections are organized as follows: Section 3.1 describes the composition of scenario files, including maneuver classes and their variants; Section 3.2 presents the characteristics of driving trajectories and explains the feature selection process; finally, Section 3.3 defines the criteria used for rule-based maneuver classification.

3.1. Dataset

In this study, a dataset was constructed for the generation of scenario based on the simulation of autonomous driving referencing the OpenSCENARIO v1.2 standard. Each scenario was designed to replicate a range of vehicle maneuvers that commonly occur in urban driving environments, and includes a total of seven maneuver types: Straight (ST), Left Turn (LT), Right Turn (RT), Left Lane Change (LLC), Right Lane Change (RLC), Roundabout Maneuvering (RA), and U-turn (UT).

Straight driving scenarios encompass not only simple straight roads but also those containing curved segments in the form of S-curve and C-curve, thus inducing diverse steering behaviors within a single maneuver type. For each scenario, variations were introduced in terms of starting and ending positions, and simulations were conducted at urban-appropriate speeds of 20, 30, 40, and 50 km/h. In the case of U-turns (UT), which involve tight maneuvering, the speed was limited to 5 and 10 km/h to reflect realistic execution conditions.

The dataset includes the following breakdown: 4 types of straight driving, 2 types of turning maneuvers, 2 types of lane changes, 3 types of roundabout maneuvering and 1 type of UT. These scenarios were further diversified by varying parameters such as traffic signal presence, vehicle speed, and start/end locations, as summarized in Table 1. In total, 1736 scenario instances were generated.

https://doi.org/10.3390/ijgi15010037

Table 1. Scenario Classes, Types, and Counts.

Scenario Class	Type	Samples
Straight	None	63
	S-curve Straight	63
	C-curve Straight (Left & Right)	126
Left Turn	None	252
Right Turn	None	252
LLC	None	252
RLC	None	252
Roundabout	3 o'clock exit	84
	12 o'clock exit	84
	9 o'clock exit	84
U-Turn	None	224

Figure 1 illustrates the visualization results of three types of straight-driving scenarios: simple straight, C-curve, and S-curve roads. The visualization was generated using a custom tool that parses OpenSCENARIO XML data and projects vehicle definitions and behaviors onto a map-based interface. In each scenario, the Ego vehicle follows a predefined road structure, and its trajectory is visually represented over a road network. Each scenario is constructed by defining the Ego vehicle and a designated stop point, with waypoints configured to guide the vehicle to its destination. A variety of scenario instances were generated at regular intervals by combining parameters such as the vehicle's initial position, destination, and speed conditions.

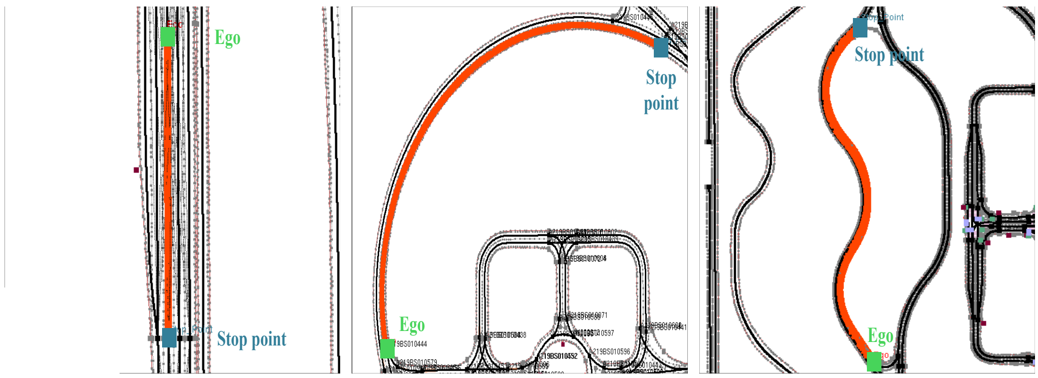

(**a**) Straight (**b**) C-curve Straight Scenario (**c**) S-curve Straight Scenario

Figure 1. Straight Scenario Trajectories in the Scenario Dataset.

The green dot represents the ego vehicle, the blue dot indicates the stop point, and the red line shows the predefined path. The visualization is taken from the scenario generation program, which also displays the surrounding road layout, allowing verification of the driving environment context.

Figure 2 presents the visualization of vehicle trajectories based on simulation results, where each scenario was executed in a virtual environment and the resulting driving data was collected. This visualization includes a total of 12 scenario types. Red dots indicate the starting points of the vehicles, while blue X-marks denote the end points. The trajectories are based on the global coordinate system of the simulator, with the origin normalized to $(0, 0)$ for visualization in a bird's-eye view. In addition, the trajectory color represents the vehicle speed, normalized against the maximum speed of the scenario, allowing the viewer to intuitively observe the speed variation during the maneuver. However, the visualization does not include detailed information about the road geometry, surrounding buildings, or environmental objects. This limitation implies that scenario classification based on road shape or environmental context is not feasible with the given data. Despite this limitation, the scenario composition was carefully designed to ensure both diversity in driving maneuvers and reproducibility in simulation conditions, making the dataset well suited for training and validation in simulation-based experiments.

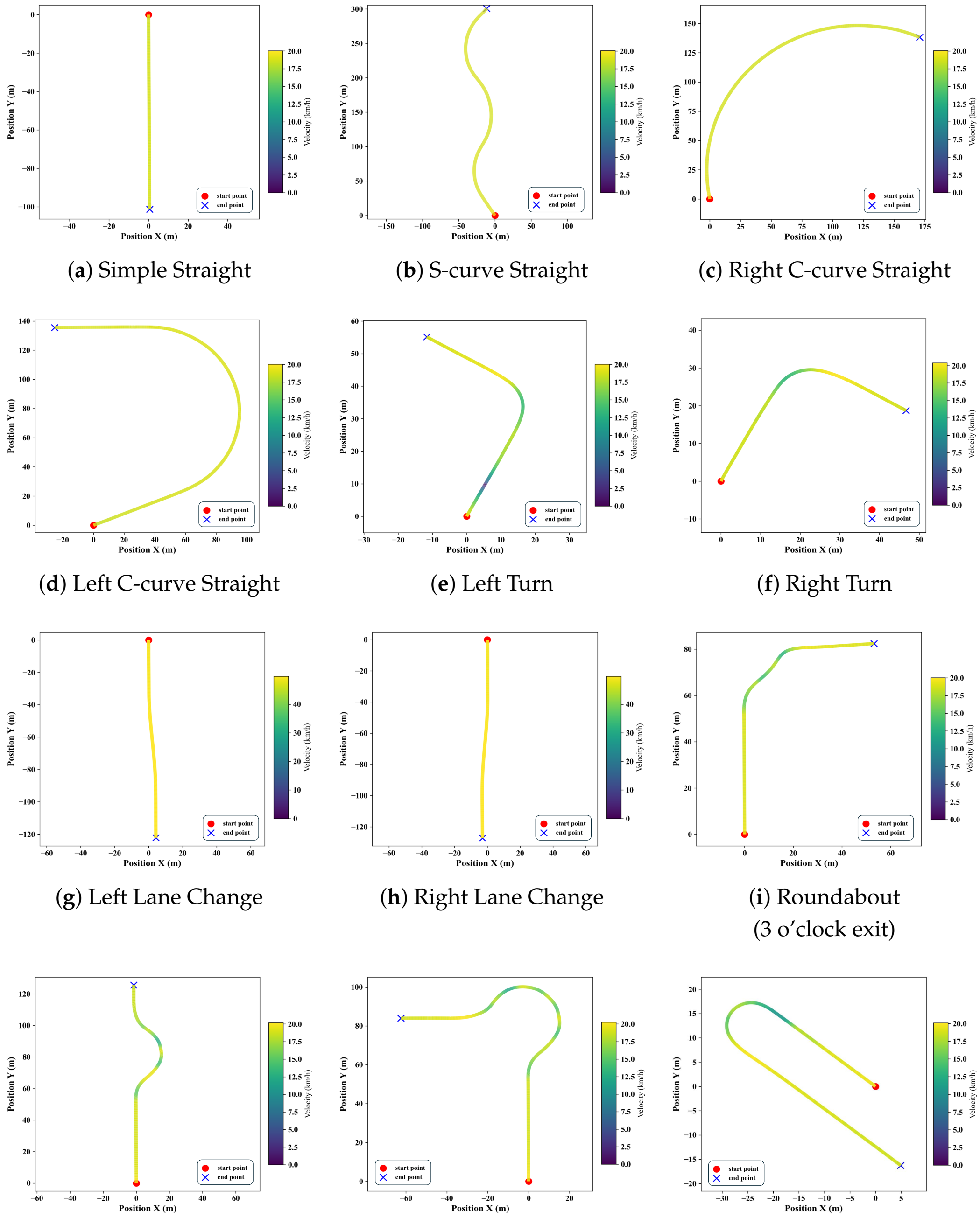

(**a**) Simple Straight (**b**) S-curve Straight (**c**) Right C-curve Straight

(**d**) Left C-curve Straight (**e**) Left Turn (**f**) Right Turn

(**g**) Left Lane Change (**h**) Right Lane Change (**i**) Roundabout (3 o'clock exit)

(**j**) Roundabout (12 o'clock exit) (**k**) Roundabout (9 o'clock exit) (**l**) U-Turn

Figure 2. Visualization of the Twelve Maneuver Scenarios Used in the Dataset. Each subfigure illustrates a representative vehicle trajectory for a specific maneuver type, where the red circle indicates the starting point and the blue "x" indicates the end point of the trajectory. The color along the trajectory denotes the vehicle's speed, normalized and represented by the accompanying color bar.

The simulation output was recorded at a frequency of 50 Hz, capturing the state information of all entities involved in each scenario. The format and structure of the recorded data are summarized in Table 2, and the key data fields are defined as follows.

Position values (X, Y, Z) are defined using the ENU (East–North–Up) coordinate system [43], where the X-, Y-, and Z-axes point east, north, and up, respectively, as shown in Figure 3a. This serves as the global coordinate system of the simulator, and the values are expressed in meters. The position represents the absolute spatial location of each object within the simulation. However, due to variations in the underlying map configurations, identical coordinate values may not correspond to identical driving paths across different scenarios. Velocity and acceleration are defined with respect to the vehicle coordinate system, where the longitudinal (X-), lateral (Y-), and vertical (Z-) axes correspond to forward, left/right, and upward directions, respectively. Velocity is measured in kilometers per hour (km/h), and acceleration in meters per second squared (m/s^2). Among these, lateral acceleration along the Y-axis is particularly significant, as it is highly responsive to turning motions, lane changes, and other maneuvering behaviors. Rotation is also defined in the vehicle coordinate system and measured in degrees. It represents the angular orientation of the vehicle around each axis, with roll corresponding to rotation around the X-axis, pitch around the Y-axis, and yaw around the Z-axis, as illustrated in Figure 3b.

Table 2. Major Features in the Driving Trajectory Dataset.

Feature	Type/Unit
Time	s (sec)
Entity	String
Position X	m
Position Y	m
Position Z	m
Velocity X (entity coordinate)	km/h
Velocity Y (entity coordinate)	km/h
Velocity Z (entity coordinate)	km/h
Acceleration X (entity coordinate)	m/s^2
Acceleration Y (entity coordinate)	m/s^2
Acceleration Z (entity coordinate)	m/s^2

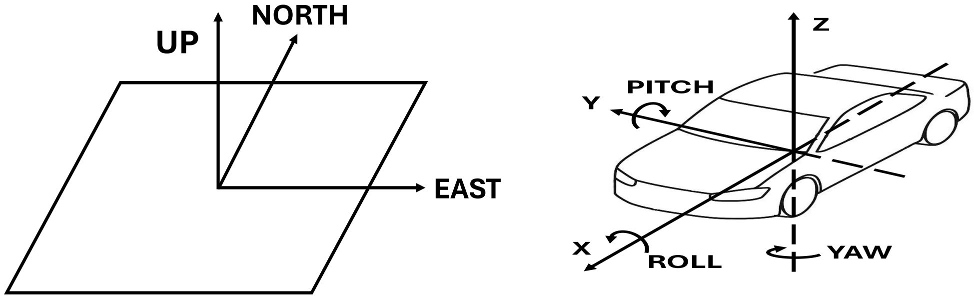

(**a**) East–North–Up (ENU) coordinate system (**b**) Vehicle Coordinate System

Figure 3. Coordinate Systems in Simulator (**a**) The ENU (East–North–Up) coordinate system represents the global reference frame used by the simulator, suitable for aligning with Earth-fixed coordinates. (**b**) The vehicle coordinate system defines the reference frame relative to the ego vehicle, where the X-axis points forward, Y-axis to the left, and Z-axis upward. Rotational movements are defined as roll (around the X-axis), pitch (around the Y-axis), and yaw (around the Z-axis), with yaw being the most relevant component for describing vehicle turning behavior.

3.2. Methodology

In this study, a rule-based classification methodology is adopted to identify driving scenarios based on vehicle motion data, with lateral acceleration (a_y) employed as the key physical indicator. The problem of driving scenario classification can be fundamentally reduced to identifying changes in driving direction, as lateral acceleration directly quantifies the dynamic response that occurs when a vehicle's trajectory changes direction.

First, lateral acceleration provides physically interpretable and distinctive patterns for differentiating maneuver types. According to prior studies, lateral acceleration—together with heading angle and velocity—exhibits characteristic signal patterns during steering behaviors such as left and right turns as well as lane changes [13,17,18,32–36,44]. In particular, research utilizing UAV-derived trajectory data has demonstrated that the correlation between lateral acceleration and speed serves as a key feature for inferring direction-changing maneuvers [45], while changes in trajectory curvature and lateral displacement rates have been shown to be essential indicators for lane-change detection [46].

In addition, lateral acceleration offers a reliable basis for defining maneuver intensity and threshold criteria. Previous studies have identified abrupt maneuvers by applying specific acceleration thresholds (e.g., 5 m/s^2) [47], or by directly using lateral acceleration values as input variables to assess maneuver validity [13,17,18]. Unlike black-box learning-based models, such physically grounded indicators enable explicit justification of classification outcomes, making them particularly well suited as features within a rule-based framework. Consequently, based on the physical insights established in previous work, this study designates lateral acceleration as the central variable for defining driving scenarios, in order to simultaneously achieve high accuracy of maneuver identification and strong interpretability of the model in complex urban driving environments.

Building on these previous studies, we further analyze the role of lateral acceleration in our dataset. As shown in Figure 4, even when vehicles start with higher initial and target speeds, the magnitude of lateral acceleration remains relatively stable due to deceleration before and during turns. This behavior is particularly evident in the 12 o'clock exit roundabout scenario, where vehicles with different initial speeds from 20 to 50 km/h at 5 km/h intervals consistently slow down before entering the turning section, resulting in similar acceleration patterns throughout the turn. This tendency to decelerate before cornering at higher speeds leads to a negative correlation between speed and acceleration, reinforcing the significance of lateral acceleration as a key feature for scenario classification.

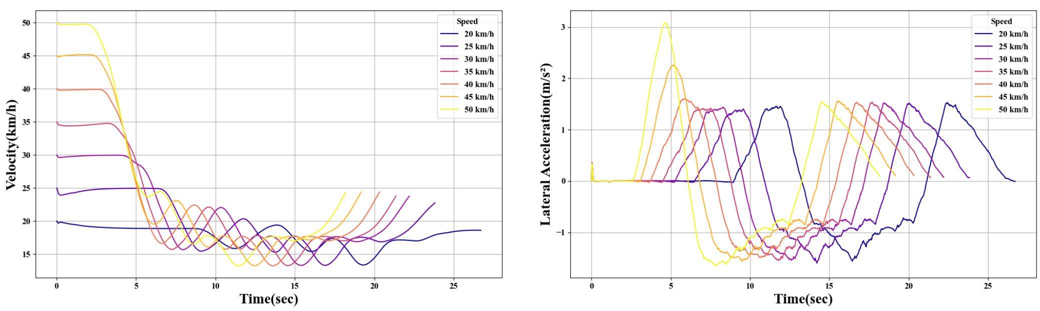

(**a**) Speed variation over time (**b**) Acceleration variation over time

Figure 4. Speed and Acceleration Variations in RA Scenarios by Velocity For the 12 o'clock exit roundabout scenario, the figures illustrate speed and acceleration variations over time according to the initial velocity. the speed graph shows intervals of 5 km/h, ranging from 20 to 50 km/h. In (**a**), It can be observed that the speed uniformly decreases to around 20 km/h upon entering the turning section. In (**b**), the acceleration profiles over time for each initial speed indicate similar acceleration patterns during the turning phase, as the speed decreases in all cases.

Based on these insights, our study adopts lateral acceleration thresholds as the primary criterion for scenario classification. The proposed maneuver types are aligned with simulation-based driving scenarios and are defined as follows, based on vehicle behavior and trajectory geometry:

- Straight (ST): Driving along a lane without directional changes, including both straight and curved roads.
- Left Turn (LT): Turning left at a four-way intersection, typically from the leftmost lane to the corresponding leftward exit lane.
- Right Turn (RT): Turning right from the rightmost lane at the same type of intersection.
- Left/Right Lane Change (LLC/RLC): Changing to the adjacent left or right lane during straight driving, followed by alignment to the forward direction.
- Roundabout (RA): Entering a roundabout and exiting along a clockwise path covering the 3 o'clock, 12 o'clock, and 9 o'clock directions.
- U-Turn (UT): Performing a U-turn on a three-lane road without reversing.

Each maneuver is classified based on the characteristics of lateral acceleration. However, in the case of straight driving, scenarios may involve variations in lateral acceleration beyond typical straight-line motion. Therefore, assuming only minimal lateral acceleration is insufficient for accurate classification. To address this, straight driving scenarios were further subdivided into three categories based on the following criteria:

1. Low lateral acceleration across the trajectory (i.e., consistent forward motion).
2. Consistent lateral acceleration during curved driving segments.
3. Repeated lateral oscillation in S-shaped roads, where the vehicle maintains significant lateral acceleration for extended durations.

In some cases, particularly for the third type of straight-driving scenarios, the vehicle's trajectory may resemble that of a roundabout maneuvering (RA), depending on its entry direction and speed. To avoid potential misclassification, appropriate threshold values must be carefully defined. For instance, on a left C-curve road segment classified as straight driving, the vehicle may exhibit sustained leftward lateral acceleration over a certain period, a characteristic also observed in RA maneuvers when the vehicle exits toward the 12 o'clock or 9 o'clock direction. LT and RT scenarios may involve either stop-and-go movement due to traffic signals or continuous turns without stopping. When a stop occurs, it is assumed that the vehicle halts at the designated stop line, with no notable lateral acceleration observed before the stop. Dynamically, LT maneuvers typically feature a larger turning radius and higher speed than RT maneuvers, which are usually executed at lower speeds and within tighter curves. Despite these differences, both scenarios involve abrupt changes in direction, producing distinct patterns in lateral acceleration that enable reliable classification. Consequently, LT and RT maneuvers are best classified after filtering out other scenario types to minimize ambiguity and enhance robustness. Lane change maneuvers (LLC and RLC) involve lateral displacement followed by directional realignment, resembling typical highway or urban driving behaviors. The magnitude and duration of lateral acceleration in such maneuvers are influenced by both the distance of the lane change and the vehicle's speed. RA maneuvers consist of a sequence of directional changes (rightward entry, circular motion, and rightward exit) forming a compound behavior of right turn, leftward progression, and another right turn. The unique pattern of lateral acceleration associated with this sequence is used to identify RA scenarios. Finally, UT maneuvers are defined by large-radius leftward turns that result in significantly greater lateral acceleration than LT maneuvers; accordingly, a higher threshold is applied to distinguish UT from other types.

3.3. Data Analysis and Rules

Figure 5 presents the visualization of lateral acceleration (Y-axis) data collected through the simulator for the 12 driving scenarios defined in this study. The horizontal axis represents time (in seconds), while the vertical axis indicates the magnitude of lateral acceleration. Positive values correspond to rightward turns, whereas negative values indicate leftward turns. The data were recorded at a sampling rate of 50 Hz and smoothed using a 100-point rolling average, effectively yielding a 2 s moving average to mitigate noise.

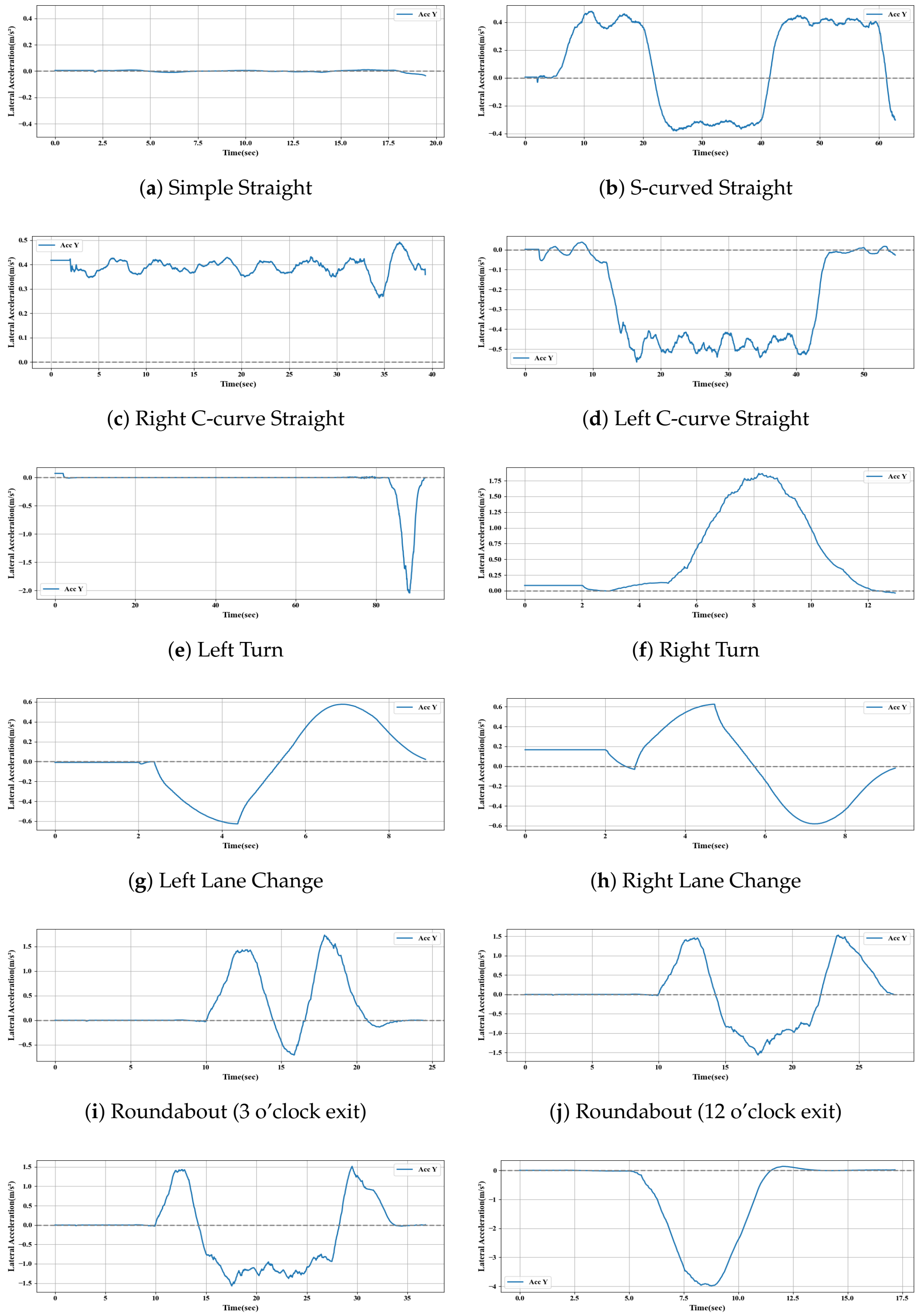

(**a**) Simple Straight (**b**) S-curved Straight

(**c**) Right C-curve Straight (**d**) Left C-curve Straight

(**e**) Left Turn (**f**) Right Turn

(**g**) Left Lane Change (**h**) Right Lane Change

(**i**) Roundabout (3 o'clock exit) (**j**) Roundabout (12 o'clock exit)

(**k**) Roundabout (9 o'clock exit) (**l**) U-Turn

Figure 5. Time-series Visualization of Lateral Acceleration for Each of the Twelve Driving Scenarios. The horizontal axis represents time in seconds, and the vertical axis represents lateral acceleration (m/s^2). This acceleration corresponds to the plots at the minimum speed of each scenario. Each plot illustrates the distinct lateral acceleration pattern corresponding to a specific maneuver. The dashed horizontal line indicates zero lateral acceleration.

According to the visualization, LT and RT scenarios exhibit a distinct single-phase lateral acceleration pattern in the respective directions.It was observed that even at a low speed of 20 km/h, the absolute value of lateral acceleration can exceed 1.5 m/s^2, typically occurring over a relatively short duration of approximately 6 s. This pattern was also observed in LT maneuvers, particularly when the vehicle starts moving again after a temporary stop due to traffic signals. These consistent acceleration signatures suggest that turning maneuvers can be effectively identified using relatively simple rule-based thresholds. In contrast, lane changes, roundabout maneuvers, and curved straight-driving scenarios tend to exhibit multiple lateral acceleration events over time, indicating more complex dynamic behavior. Considering these differences, it is more effective to establish classification rules based not only on peak acceleration values but also on the magnitude and duration of acceleration patterns. For example, lateral acceleration changes that last less than 8 s are likely to correspond to short, distinct maneuvers such as turns or lane changes. In contrast, sustained acceleration patterns over 10 s are more indicative of continuous curved-road driving. Similarly, a pattern involving right–left–right turning maneuvers within 30 s is rarely observed in typical driving but is commonly found in roundabout scenarios.

Based on these insights, simpler rules were defined for scenario types with distinct characteristics, while more complex scenarios were classified using a combination of factors such as the duration, magnitude, and temporal order of lateral acceleration. Thresholds and parameters (i.e., minimum acceleration and required duration) were carefully selected to maximize coverage across diverse scenarios, enabling generalized rule-based classification for each class. For example, in turning scenarios, it was observed that lower driving speeds tend to result in smaller lateral acceleration compared to other turning maneuvers. To address this, data analysis revealed that the absolute value of lateral acceleration rarely falls below 1.0 m/s^2 during actual turning. Accordingly, a minimum threshold of 1.0 m/s^2 (absolute) was applied to avoid misclassifying low-acceleration segments as turns. In addition, a minimum duration of 3 s was enforced, reflecting the time typically required for a turning maneuver to take place. This approach was similarly applied to other types of scenario trajectories, allowing for a generalized and consistent rule-based classification framework. The detailed rule definitions are presented in the following:

- Straight: During normal driving, the absolute value of lateral acceleration must remain below 0.05 m/s^2 throughout the entire segment. When driving on a curved road, all subsequent values must remain within 0.1 m/s^2 relative to the initial lateral acceleration. If the lateral acceleration exceeds 0.3 m/s^2, it must persist for at least 8 s to be considered a curved straight scenario.
- Turn (RT and LT): A lateral acceleration greater than $+1.0$ m/s^2 (for RT) or lower than -1.0 m/s^2 (for LT) must be sustained for at least 3 s.
- Lane Change (LLC/RLC): The absolute value of lateral acceleration must exceed a threshold of 0.2 m/s^2 and remain above it for at least 0.7 s. Lane change classification is based on the temporal sequence of lateral acceleration events, including their direction and spacing.
- Roundabout (RA): At least one event must exhibit lateral acceleration exceeding 0.3 m/s^2 in magnitude for more than 1.3 s. The detected events must follow the sequential pattern of right–left–right turns. The left-turn segment must not exceed a maximum duration of 15 s, to prevent confusion with U-turns or prolonged curved driving.
- U-Turn (UT): Lateral acceleration must drop below -3.0 m/s^2 and remain below this threshold for at least 2 s.

The thresholds were set as low as possible to ensure generalization. In particular, due to the nature of vehicle acceleration data, the magnitude varies depending on speed even when following the same path. That is, when changing direction at higher speeds, greater acceleration occurs in proportion to the speed. Considering this characteristic, the thresholds for class separation were determined based on low-speed driving data for each scenario. As illustrated in Figure 5 for the ST case, typical straight driving does not exceed an absolute lateral acceleration of 0.05 m/s^2 even at higher speeds (Minimum: −0.0449, Maximum: 0.0268). In contrast, S-curve driving exhibits absolute lateral acceleration values exceeding 0.3 m/s^2 in both right and left turns, and the effect persists for a relatively longer duration than RT or LT maneuvers. To distinguish such maneuvers from other turning actions, an additional threshold of at least 8 s of duration was introduced. The same phenomenon was observed in RRST and LRST scenarios, and thus, the same criteria were applied. Using this approach, threshold values for other maneuver classes were also determined. However, as these thresholds were manually defined by the researcher, they may not represent the optimal parameters. This limitation and the parameter optimization process will be further discussed in Section 4.2.

4. Experimental Results

This section presents the results of scenario classification based on the previously described rule-based conditions. It first addresses the issue of overlapping class assignments, where a single scenario may be classified into multiple maneuver types due to shared rule conditions. To resolve this problem, we explored and established rule priorities to eliminate redundant classifications. Finally, recognizing the limitations of manually set parameters, we conducted a parameter optimization process to further improve performance.

4.1. Observed Issues During Inference

The results of maneuver classification based on the proposed rule-based conditions are presented in Table 3. This table illustrates how each rule applies to individual scenarios, allowing identification of which classification conditions are satisfied by each case. For example, a roundabout (RA) scenario may fulfill not only the RA rule but also those associated with ST, UT, LT, or RLC, indicating that a single scenario can correspond to multiple maneuver classes. Conversely, scenarios that do not meet any of the defined rules are assigned to the UL (Unlabeled) class. As shown in Table 3, rule-based classification without post-processing may result in ambiguous labeling, where a single scenario is mapped to multiple classes. This overlap highlights the limitation of using rule-based methods alone for exclusive class identification.

Table 3. Label Matrix for Scenario Classification without Priority.

Real	Prediction								Samples
	RA	ST	UT	LT	RT	LLC	RLC	UL	
RA	240	84	0	168	0	0	252	0	252
ST	54	243	0	81	63	9	0	2	252
UT	0	0	224	224	0	197	0	0	224
LT	0	0	0	252	0	52	0	0	252
RT	0	0	0	0	252	0	0	0	252
LLC	0	0	1	1	0	252	0	0	252
RLC	0	0	0	0	0	0	252	0	252

UL (unlabeled) denotes scenarios that do not satisfy the conditions of any predefined maneuver class.

In this approach, rules with narrower scope or stronger discriminatory power should be applied earlier, while more general rules (e.g., those for LT and RT, which tend to match a wide range of turning behaviors) should be applied later in the sequence. These broader rules, though effective in capturing turning maneuvers, may lack the specificity needed to distinguish between fine-grained behavior types. To address this issue, an additional experiment was conducted to determine an optimal rule application order based on classification performance.

4.2. Extended Experiments for Problem Resolution

To determine the rule application order that yields the highest score, we conducted experiments on all possible permutations. This process corresponds to the priority search and configuration stage indicated by the red blocks in Figure 6. In total, all 7! (=5040) permutations were tested and the evaluation was performed using F1-score. After analyzing the results for all permutations, the top 16 priority sequences with the highest F1-scores in the manual parameter are presented in Table 4. These represent the best-performing rule orders among the 5040 permutations. From the sequences listed in Table 4, it can be observed that more fine-grained rules (RA, ST, UT) tend to appear earlier in the order. In particular, RA consistently shows the highest priority, likely because it represents one of the most distinctive driving behavior patterns. Specifically, the characteristics of RA involve acceleration patterns in the sequence of right–left–right movements, while RT, RLC, LC, and LLC are often detected within portions of this RA trajectory. These priority orders are based on manually set parameters and may change in future optimization. Among them, a single representative order was selected, corresponding to the first sequence presented in the Table 4. Parameter optimization will be discussed in the following paragraph.

Table 4. Rule Priority Orders with the Highest Matching Scores.

No.	Rule1	Rule2	Rule3	Rule4	Rule5	Rule6	Rule7
1	RA	ST	UT	LT	RT	LLC	RLC
2	RA	ST	UT	LT	RT	RLC	LLC
3	RA	UT	ST	LT	RT	LLC	RLC
4	RA	UT	ST	LT	RT	RLC	LLC
5	RA	UT	ST	LT	LLC	RT	RLC
6	RA	UT	ST	LT	LLC	RLC	RT
7	RA	UT	ST	LT	RLC	RT	LLC
8	RA	UT	ST	LT	RLC	LLC	RT
9	RA	UT	ST	RT	LT	LLC	RLC
10	RA	UT	ST	RT	LT	RLC	LLC
11	RA	ST	UT	LT	LLC	RT	RLC
12	RA	ST	UT	LT	LLC	RLC	RT
13	RA	ST	UT	LT	RLC	RT	LLC
14	RA	ST	UT	LT	RLC	LLC	RT
15	RA	ST	UT	RT	LT	LLC	RLC
16	RA	ST	UT	RT	LT	RLC	LLC

Using manually tuned parameters based on trajectory information, the classification achieved an accuracy of 0.9510 and an F1-score of 0.9515, as shown in Table 5. These results demonstrate that the classification approach that uses lateral acceleration (y-axis) has a significant impact on the identification of vehicle behaviors. Although most classes exhibit high recall values, the ST class shows a relatively low recall of 0.75. In addition, some instances were misclassified across different classes.

To overcome these issues, we used the Optuna framework to optimize parameters dynamically instead of setting them manually. We employed the framework to dynamically search for optimal parameters within a predefined range, allowing for more efficient exploration compared to other optimization methods [48,49]. The Optuna framework was applied in the yellow blocks shown in Figure 6. Recognizing that the results varied depending on the priority of the rules we defined, we repeated the parameter optimization, priority search, and assignment processes three times. The final outcomes obtained from these iterations are presented in Table 6. As shown in Table 6, most classes were successfully distinguished. The model achieved an accuracy of 0.9784, a recall of 0.9745, and an F1-score of 0.9764, which are higher than those obtained with manually configured parameters. In the optimized parameters and priority settings as shown in Table 7, RA maintained the highest priority, as observed in Table 5, while the priorities of the other classes changed.

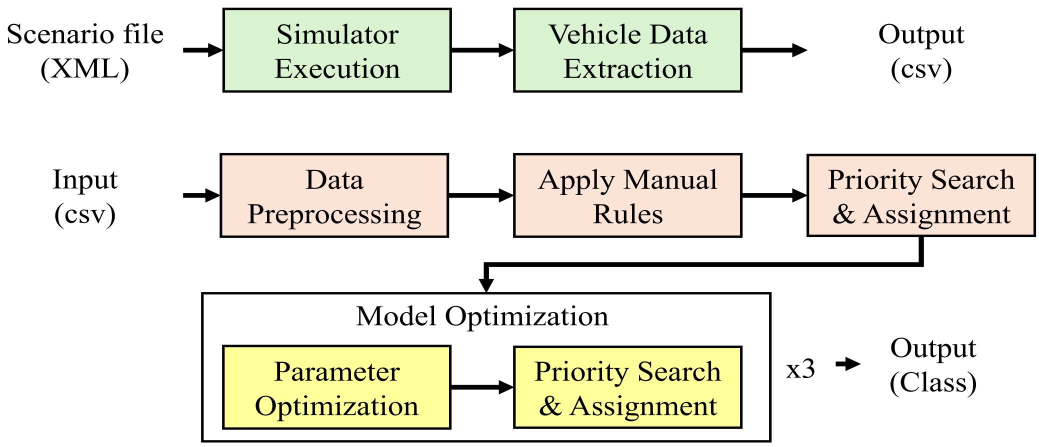

Figure 6. Research Flowchart. The figure divides the research procedure into three sections: data extraction, manual rule configuration, and parameter optimization. The green block represents data extraction, where the simulator's physical engine processes XML-defined scenario files (.xosc) to obtain vehicle position, speed, and acceleration data. The red block shows the analysis of driving data, defining manual rules and parameters and assigning corresponding priorities. The yellow block depicts parameter optimization. The framework sets a search range based on manually defined parameters and repeats the training three times while considering priority-based variations to obtain the final model.

Table 5. Confusion Matrix with Manually Set Parameters.

Real	**Prediction**								**Samples**
	RA	**ST**	**UT**	**LT**	**RT**	**LLC**	**RLC**	**UL**	
RA	240	0	0	0	0	0	12	0	252
ST	54	189	0	0	0	0	0	9	252
UT	0	0	224	0	0	0	0	0	224
LT	0	0	0	252	0	0	0	0	252
RT	0	9	0	0	243	0	0	0	252
LLC	0	1	0	0	0	251	0	0	252
RLC	0	0	0	0	0	0	252	0	252
Total	294	199	224	252	243	251	264	9	1736

UL (unlabeled) denotes scenarios that do not satisfy the conditions of any predefined maneuver class.

Table 6. Confusion Matrix with Optimized Parameters.

Real	**Prediction**								**Samples**
	RA	**UT**	**LT**	**RT**	**ST**	**LLC**	**RLC**	**UL**	
RA	252	0	0	0	0	0	0	0	252
UT	0	224	0	0	0	0	0	0	224
LT	0	0	252	0	0	0	0	0	252
RT	0	0	0	252	0	0	0	0	252
ST	45	0	0	0	207	0	0	0	252
LLC	0	0	0	0	0	252	0	0	252
RLC	0	0	0	0	0	0	252	0	252
Total	297	224	252	252	207	252	252	0	1736

UL (unlabeled) denotes scenarios that do not satisfy the conditions of any predefined maneuver class.

Table 7. Optimized Parameter Set.

Class	Parameter Name	Value
LLC	llc_min_threshold	0.21236
	llc_min_duration_sec	0.87535
RLC	rlc_min_threshold	0.13783
	rlc_min_duration_sec	0.83308
ST	st_zero_abs_threshold	0.07793
	st_rotation_abs_threshold	0.99754
	st_min_duration_sec	7.53244
RT	rt_min_right_threshold	1.18379
	rt_min_duration_sec	1.57470
	rt_max_duration_sec	5.47996
LT	lt_min_left_threshold	−0.42793
	lt_min_duration_sec	4.13702
	lt_max_duration_sec	6.15622
RA	ra_negative_threshold	−0.14637
	ra_positive_threshold	0.09736
	ra_min_duration_sec	1.45499
	ra_max_duration_sec	14.44937
UT	ut_min_threshold	−2.18747
	ut_min_duration_sec	2.82387

Parameter values used in the optimized maneuver detection configuration.

For each of the seven maneuver classes as shown in Table 7, the variables primarily consist of two common elements: the minimum threshold and the minimum duration. The minimum threshold determines the detectability of a maneuver when the measured value exceeds or falls below a certain limit. Specifically, for RT trajectories, the threshold corresponds to values exceeding a positive limit, while for LT trajectories, it corresponds to values below a negative limit. In the case of ST, the lateral acceleration maintains a constant value and both the initial and sustained threshold values are identical. The ST parameters are composed of the rotation-related value and the duration for which the rotation is maintained. Similarly, for RA (Roundabout trajectory), separate thresholds are defined for right and left rotations, each with its own minimum and maximum duration. Although the rule-based trajectory classification model achieved an F1-score of 0.9764 using these parameters, the thresholds themselves do not necessarily represent optimal boundary values. For example, in the case of the UT, the previous configuration used a threshold of -3.0 m/s^2 and a duration of 2 s, producing a similar level of performance. This indicates that the parameters do not always correspond to globally optimal values. Although the optimization process used the Optuna framework, the discontinuity of the objective function likely led to the discovery of these parameter sets through random-space exploration rather than true global optimization.

4.3. Results

To validate the practical utility of the proposed method, a supplementary comparative experiment was conducted against a basic RNN baseline and the LSTM architecture adopted in [17], with an emphasis on computational efficiency and practical applicability. All models were evaluated under identical conditions, using the same preprocessing to that of the rule-based classifier, without additional calibration for time-series length.

As summarized in Table 8, the rule-based classifier demonstrated substantially faster processing speeds than both the RNN and LSTM models, reflecting its structurally simple and computationally lightweight design. In terms of classification performance, the rule-based method achieved higher accuracy and an F1-score superior to the RNN baseline, while showing slightly lower performance than the LSTM model. These results indicate that the proposed rule-based framework serves as a practical and efficient lightweight baseline for simulation pipelines requiring large-scale scenario evaluation. In addition, unlike deep-learning-based approaches that operate as "black boxes," the rule-based method provides clear interpretability, allowing classification decisions to be explicitly examined and visualized.To demonstrate this transparency, Figure 7 visualizes the classification logic for specific classes through masking. This visualization is crucial because certain maneuvers, such as Roundabout (RA), S-curve, and Straight (ST), exhibit strikingly similar lateral acceleration profiles, as shown in Figure 8. By providing such visual evidence, the proposed framework ensures that the underlying physical rationale for distinguishing these ambiguous cases is fully transparent and verifiable.

Notably, the LSTM model achieved strong classification performance despite relying solely on lateral acceleration as the input feature. This observation reinforces the premise that lateral acceleration alone encodes sufficient information for distinguishing driving maneuvers, provided that temporal dependencies are effectively captured. Accordingly, these findings validate that lateral acceleration functions as a informative core feature for both rule-based logic and learning-based architectures.

In summary, the comparative analysis highlights a distinct trade-off between computational efficiency and discriminative power. While the rule-based framework offers exceptional speed and transparency, learning-based models like LSTM provide enhanced performance at the cost of increased computational burden. These insights provide a quantitative basis for selecting an appropriate classification strategy depending on the specific requirements of the autonomous driving validation task.

Table 8. Comparison of the Proposed Rule-based Model and Deep Learning Models.

Model	Accuracy (%)	F1-Score (%)	Rate (Samples/s)
RNN	0.2661	0.1676	29.06
LSTM	0.9856	0.9855	29.96
Proposed Model	0.9741	0.9764	74.72

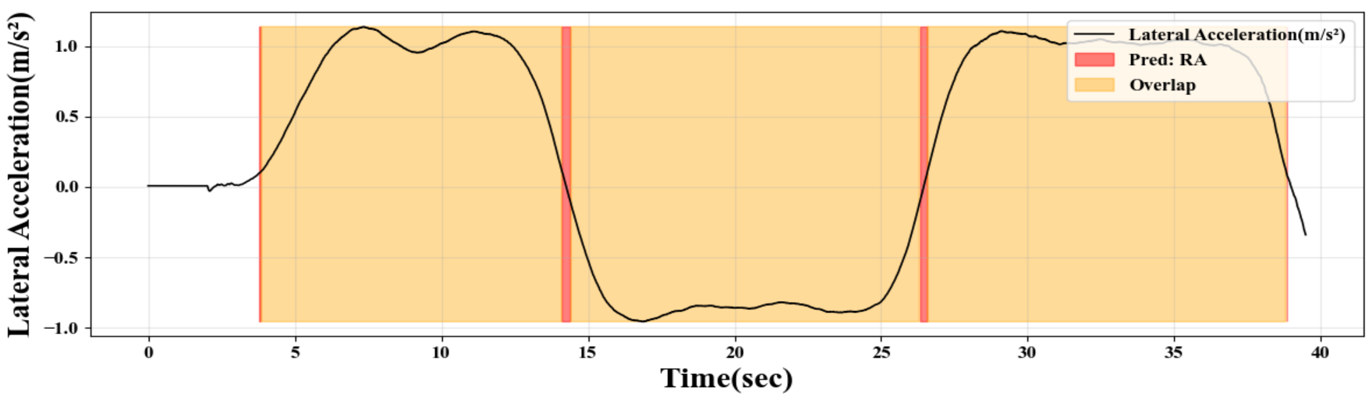

Figure 7. Visualization of Misclassification from S-shape Straight to Roundabout. This figure visualizes the section where the S-shape Straight is classified as a Roundabout. The data indicate that the model detects a long period of acceleration in one direction, which is characteristic of a Straight scenario, while also capturing the alternating right–left–right acceleration pattern that typically appears in a Roundabout.

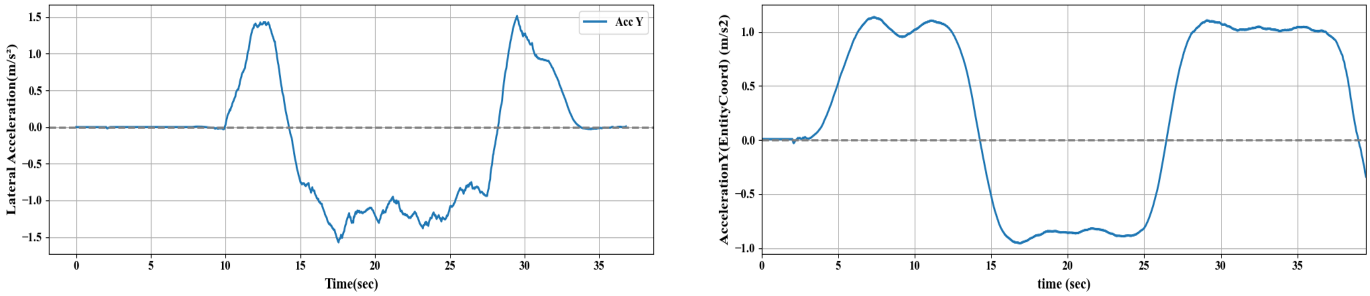

(**a**) Roundabout (9 o'clock exit) (**b**) S-curve Straight

Figure 8. Comparison of Lateral Acceleration between the Roundabout (9 o'clock exit) and S-curve Straight Scenarios. The dashed horizontal line indicates zero lateral acceleration.

5. Discussion

The findings of this study provide critical insights into the balance between interpretability and classification performance, while also highlighting areas for further refinement in scenario-based validation.

5.1. Structural Limitations and the Need for Hybrid Modeling

The structural limitations of the rule-based approach must be addressed. While the proposed classifier is highly efficient, it encounters challenges when maneuver classes exhibit nearly identical lateral acceleration patterns. Because the classification logic relies on a constrained set of handcrafted physical features, it lacks the inherent flexibility to integrate high-dimensional kinematic cues, such as trajectory curvature or subtle variations in heading. Consequently, scenarios with overlapping dynamic characteristics remain difficult to distinguish under a purely rule-based framework. This suggests that while rule-based logic is ideal for high-level filtering, it may require augmentation from more sophisticated models to resolve fine-grained ambiguities.

5.2. Scalability to Real-World Traffic Dynamics

Regarding the transition from simulated to real-world data, this study lays a foundational framework for automated scenario indexing. Previous literature [11–15] underscores the importance of structuring real-world driving data into reusable scenario units. However, several considerations remain before this approach can be fully deployed in complex real-world environments. A primary constraint of the current dataset is the absence of interaction with other traffic participants. As noted in prior studies [11–15,42,50,51], the presence of surrounding vehicles significantly influences the duration and timing of maneuvers (i.e., such as lane changes or turns) due to required stops or yielding behaviors. Future iterations of the framework must incorporate these interactive dynamics to ensure that the classified scenarios accurately reflect the stochastic nature of real-world traffic.

5.3. Dataset Characteristics and Learning Stability

The characteristics of the dataset itself pose challenges for broader machine learning applications. As illustrated in Figure 9, the current dataset exhibits a degree of class imbalance, which acts as a constraint for conducting extensive experiments across diverse deep learning architectures. Such imbalance can hinder stable model training and lead to inconsistent performance metrics, particularly for underrepresented maneuver classes. To mitigate this, future work will focus on expanding the dataset and implementing data augmentation techniques to achieve a more balanced class distribution, thereby enabling a more robust and statistically significant comparative analysis.

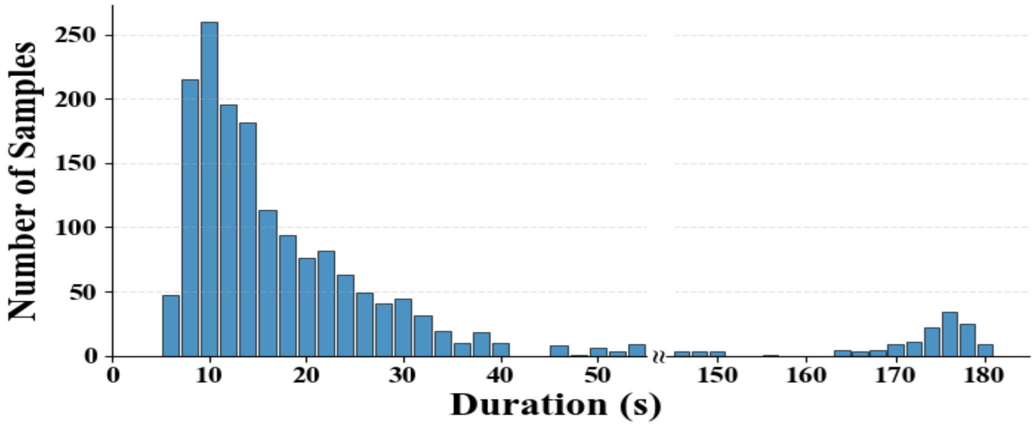

Figure 9. Distribution of Dataset Sample Lengths. This figure illustrates the length distribution of the dataset used in this study. Most samples are approximately 30 s long, while about 10% exceed 40 s. The longer samples primarily correspond to situations where vehicles wait at left-turn signals, which introduces challenges for training deep learning models.

5.4. Simulator Dependency and Cross-Platform Consistency

Differences in simulation outcomes may arise depending on the specific simulator used to execute a given scenario. Several simulation platforms support the ASAM OpenSCENARIO standard, including CARLA (https://carla.org/ (acessed on 9 January 2026)), esmini (https://esmini.github.io/ (acessed on 9 January 2026)), dSPACE-AURELION (https://www.dspace.com/ (acessed on 9 January 2026)), MORAI (https://www.morai.ai/ (acessed on 9 January 2026)), and Autoware (https://autoware.org/ (acessed on 9 January 2026)) [52]. Because each simulator implements its own internal vehicle dynamics models and physics engines, the resulting trajectory data and vehicle responses may vary across platforms, even when the same scenario specification is applied. Consequently, for consistent scenario classification and evaluation, it is necessary to fix a single simulation environment and conduct all experiments within that platform.

6. Conclusions

This study introduces a rule-based classification framework designed to identify maneuver-level scenarios within autonomous driving simulations. By leveraging lateral acceleration patterns extracted from trajectory data, the proposed method categorizes seven representative urban maneuvers through a prioritized sequence of handcrafted rules. Achieving an accuracy of 0.9784 and an F1-score of 0.9764, the framework demonstrates that a trajectory-driven, rule-based approach provides an accurate and highly interpretable solution for automated scenario labeling in simulation-based validation pipelines.

A significant contribution of this work lies in the establishment of a scalable validation environment compliant with the international OpenSCENARIO standard, specifically optimized for autonomous driving learning. Beyond mere categorization, this framework enables a quantitative assessment of driving performance across distinct scenario classes. This capability allows developers to precisely identify specific vulnerabilities in autonomous agents, particularly in complex maneuvers or edge-case navigation. By providing an interpretable classification of these performance gaps, the system serves as a strategic foundation for targeted data augmentation and retraining, directly addressing data imbalance and systematically hardening the system's safety and generalization.

Moving forward, we aim to evolve this framework into a comprehensive scenario architecture that incorporates intricate risk factors. Future research will focus on transitioning from manually defined thresholds to hybrid models—integrating decision trees and time-series deep learning—to enhance classification robustness while preserving the transparency of rule-based logic. Ultimately, this integration will support the development of sophisticated simulation environments that accurately reflect the complex and stochastic demands of real-world autonomous driving.

Author Contributions: Conceptualization, Sungmo Ku; methodology, Sungmo Ku; software, Sungmo Ku; validation, Jinho Lee; investigation, Sungmo Ku; writing—original draft preparation, Sungmo Ku; writing—review and editing, Sungmo Ku and Jinho Lee; visualization, Sungmo Ku; supervision, Jinho Lee; project administration, Jinho Lee; funding acquisition, Jinho Lee. All authors have read and agreed to the published version of the manuscript.

Funding: This work was supported by the Institute of Information Communications Technology Planning Evaluation (IITP)-Innovative Human Resource Development for Local Intellectualization program grant funded by the Korea government (MSIT) (IITP-2026-RS-2020-II201741).

Data Availability Statement: Data Availability Statement: The data supporting the findings of this study are not publicly available due to security concerns related to sensitive geographic information.

Conflicts of Interest: The funders had no role in the design of the study; in the collection, analyses, or interpretation of data; in the writing of the manuscript; or in the decision to publish the results.

References

1. Gao, C.; Wang, G.; Shi, W.; Wang, Z.; Chen, Y. Autonomous Driving Security: State of the Art and Challenges. *IEEE Internet Things J.* **2022**, *9*, 7572–7595. [CrossRef]
2. Barabás, I.; Todoruţ, A.; Cordoş, N.; Molea, A. Current Challenges in Autonomous Driving. *IOP Conf. Ser. Mater. Sci. Eng.* **2017**, *252*, 012096. [CrossRef]
3. Liu, L.; Lu, S.; Zhong, R.; Wu, B.; Yao, Y.; Zhang, Q.; Shi, W. Computing Systems for Autonomous Driving: State of the Art and Challenges. *IEEE Internet Things J.* **2021**, *8*, 6469–6486. [CrossRef]
4. Bock, F.; Sippl, C.; Heinz, A.; Lauer, C.; German, R. Advantageous Usage of Textual Domain-Specific Languages for Scenario-Driven Development of Automated Driving Functions. In Proceedings of the 2019 IEEE International Systems Conference (SysCon), Orlando, FL, USA, 8–11 April 2019; IEEE: Piscataway, NJ, USA, 2019; pp. 1–8. [CrossRef]
5. *ISO 26262:2018*; Road Vehicles—Functional Safety. International Organization for Standardization: Geneva, Switzerland, 2018.
6. *ISO/PAS 21448:2019*; Road Vehicles—Safety of the Intended Functionality (SOTIF). International Organization for Standardization: Geneva, Switzerland, 2019.
7. Chang, C.; Cao, D.; Chen, L.; Su, K.; Su, K.; Su, Y.; Wang, F.-Y.; Wang, J.; Wang, P.; Wei, J.; et al. MetaScenario: A Framework for Driving Scenario Data Description, Storage and Indexing. *IEEE Trans. Intell. Veh.* **2023**, *8*, 1156–1175. [CrossRef]
8. Scholtes, M.; Westhofen, L.; Turner, L.R.; Lotto, K.; Schuldes, M.; Weber, H.; Wagener, N.; Neurohr, C.; Bollmann, M.H.; Kortke, F.; et al. 6-Layer Model for a Structured Description and Categorization of Urban Traffic and Environment. *IEEE Access* **2021**, *9*, 59131–59147. [CrossRef]
9. Hartjen, L.; Philipp, R.; Schuldt, F.; Howar, F.; Friedrich, B. Classification of Driving Maneuvers in Urban Traffic for Parametrization of Test Scenarios. In Proceedings of the 9. Tagung Automatisiertes Fahren, Munich, Germany, 21–22 November 2019.
10. Bagschik, G.; Menzel, T.; Maurer, M. Ontology Based Scene Creation for the Development of Automated Vehicles. In Proceedings of the 2018 IEEE Intelligent Vehicles Symposium (IV), Changshu, China, 26–30 June 2018; IEEE: Piscataway, NJ, USA, 2018; pp. 1813–1820. [CrossRef]
11. de Gelder, E.; Manders, J.; Grappiolo, C.; Paardekooper, J.-P.; den Camp, O.O.; Schutter, B.D. Real-World Scenario Mining for the Assessment of Automated Vehicles. In Proceedings of the 2020 IEEE 23rd International Conference on Intelligent Transportation Systems (ITSC), Rhodes, Greece, 20–23 September 2020; pp. 1–8. [CrossRef]
12. Tenbrock, A.; Konig, A.; Keutgens, T.; Weber, H. The ConScenD Dataset: Concrete Scenarios from the highD Dataset According to ALKS Regulation UNECE R157 in OpenX. In Proceedings of the 2021 IEEE Intelligent Vehicles Symposium Workshops (IV Workshops), Nagoya, Japan, 11–17 July 2021; IEEE: Piscataway, NJ, USA, 2021; pp. 174–181. [CrossRef]
13. Karunakaran, D.; Berrio, J.S.; Worrall, S.; Nebot, E. Parameterisation of lane-change scenarios from real-world data. In Proceedings of the 2022 IEEE 25th International Conference on Intelligent Transportation Systems (ITSC), Macau, China, 8–12 October 2022; IEEE: Piscataway, NJ, USA, 2022; pp. 2607–2613. [CrossRef]
14. Guo, D.; Sánchez, M.M.; De Gelder, E.; Van Der Sande, T.P.J. Scenario Extraction from a Large Real-World Dataset for the Assessment of Automated Vehicles. In Proceedings of the 2023 IEEE 26th International Conference on Intelligent Transportation Systems (ITSC), Bilbao, Spain, 24–28 September 2023; IEEE: Piscataway, NJ, USA, 2023; pp. 1570–1575. [CrossRef]

15. Krajewski, R.; Bock, J.; Kloeker, L.; Eckstein, L. The highD Dataset: A Drone Dataset of Naturalistic Vehicle Trajectories on German Highways for Validation of Highly Automated Driving Systems. In Proceedings of the 2018 21st International Conference on Intelligent Transportation Systems (ITSC), Maui, HI, USA, 4–7 November 2018; IEEE: Piscataway, NJ, USA, 2018; pp. 2118–2125. [CrossRef]
16. Ulbrich, S.; Menzel, T.; Reschka, A.; Schuldt, F.; Maurer, M. Defining and Substantiating the Terms Scene, Situation, and Scenario for Automated Driving. In Proceedings of the 2015 IEEE 18th International Conference on Intelligent Transportation Systems, Gran Canaria, Spain, 15–18 September 2015; IEEE: Piscataway, NJ, USA, 2015; pp. 982–988. [CrossRef]
17. Aboah, A.; Adu-Gyamfi, Y.; Gursoy, S.V.; Merickel, J.; Rizzo, M.; Sharma, A. Driver Maneuver Detection and Analysis using Time Series Segmentation and Classification. *arXiv* **2022**, arXiv:2211.06463. [CrossRef]
18. Carter, N.; Beier, S.; Cordero, R. Lateral and Tangential Accelerations of Left Turning Vehicles from Naturalistic Observations. In Proceedings of the WCX SAE World Congress Experience, Detroit, MI, USA, 9–11 April 2019; p. 2019-01-0421. [CrossRef]
19. Erdogan, A.; Ugranli, B.; Adali, E.; Sentas, A.; Mungan, E.; Kaplan, E.; Leitner, A. Real-World Maneuver Extraction for Autonomous Vehicle Validation: A Comparative Study. In Proceedings of the 2019 IEEE Intelligent Vehicles Symposium (IV), Paris, France, 9–12 June 2019; IEEE: Piscataway, NJ, USA, 2019; pp. 267–272. [CrossRef]
20. Nilsson, J.; Fredriksson, J.; Coelingh, E. Rule-Based Highway Maneuver Intention Recognition. In Proceedings of the 2015 IEEE 18th International Conference on Intelligent Transportation Systems, Gran Canaria, Spain, 15–18 September 2015; IEEE: Piscataway, NJ, USA, 2015; pp. 950–955. [CrossRef]
21. Haque, M.M.; Sarker, S.; Dewan, M.A.A. Driving Maneuver Classification from Time Series Data: A Rule Based Machine Learning Approach. *Appl Intell* **2022**, *52*, 16900–16915. [CrossRef]
22. Cervantes-Villanueva, J.; Carrillo-Zapata, D.; Terroso-Saenz, F.; Valdes-Vela, M.; Skarmeta, A. Vehicle Maneuver Detection with Accelerometer-Based Classification. *Sensors* **2016**, *16*, 1618. [CrossRef] [PubMed]
23. Ferreira, J.; Carvalho, E.; Ferreira, B.V.; De Souza, C.; Suhara, Y.; Pentland, A.; Pessin, G. Driver Behavior Profiling: An Investigation with Different Smartphone Sensors and Machine Learning. *PLoS ONE* **2017**, *12*, e0174959. [CrossRef] [PubMed]
24. Wang, W.; Xi, J.; Chong, A.; Li, L. Driving Style Classification Using a Semisupervised Support Vector Machine. *IEEE Trans. Hum.-Mach. Syst.* **2017**, *47*, 650–660. [CrossRef]
25. Sarker, S.; Haque, M.M. An Approach Towards Domain Knowledge-Based Classification of Driving Maneuvers with LSTM Network. In *Proceedings of the International Joint Conference on Advances in Computational Intelligence*; Uddin, M.S., Bansal, J.C., Eds.; Algorithms for Intelligent Systems; Springer: Singapore, 2021; pp. 469–484. [CrossRef]
26. Carvalho, E.; Ferreira, B.V.; Ferreira, J.; De Souza, C.; Carvalho, H.V.; Suhara, Y.; Pentl, A.S.; Pessin, G. Exploiting the Use of Recurrent Neural Networks for Driver Behavior Profiling. In Proceedings of the 2017 International Joint Conference on Neural Networks (IJCNN), Anchorage, AK, USA, 14–19 May 2017; IEEE: Piscataway, NJ, USA, 2017; pp. 3016–3021. [CrossRef]
27. Deo, N.; Rangesh, A.; Trivedi, M.M. How Would Surround Vehicles Move? A Unified Framework for Maneuver Classification and Motion Prediction. *IEEE Trans. Intell. Veh.* **2018**, *3*, 129–140. [CrossRef]
28. Berndt, H.; Emmert, J.; Dietmayer, K. Continuous Driver Intention Recognition with Hidden Markov Models. In Proceedings of the 2008 11th International IEEE Conference on Intelligent Transportation Systems, Beijing, China, 12–15 October 2008; IEEE: Piscataway, NJ, USA, 2008; pp. 1189–1194. [CrossRef]
29. Wiest, J.; Hoffken, M.; Kresel, U.; Dietmayer, K. Probabilistic trajectory prediction with Gaussian mixture models. In Proceedings of the 2012 IEEE Intelligent Vehicles Symposium, Alcal de Henares, Madrid, Spain, 3–7 June 2012; IEEE: Piscataway, NJ, USA, 2012; pp. 141–146. [CrossRef]
30. Sarker, S.; Haque, M.M.; Dewan, M.A.A. Driving Maneuver Classification Using Domain Specific Knowledge and Transfer Learning. *IEEE Access* **2021**, *9*, 86590–86606. [CrossRef]
31. Sonka, A.; Krauns, F.; Henze, R.; Kucukay, F.; Katz, R.; Lages, U. Dual Approach for Maneuver Classification in Vehicle Environment Data. In Proceedings of the 2017 IEEE Intelligent Vehicles Symposium (IV), Los Angeles, CA, USA, 11–14 June 2017; IEEE: Piscataway, NJ, USA, 2017; pp. 97–102. [CrossRef]
32. Aoude, G.S.; Desaraju, V.R.; Stephens, L.H.; How, J.P. Behavior Classification Algorithms at Intersections and Validation Using Naturalistic Data. In Proceedings of the 2011 IEEE Intelligent Vehicles Symposium (IV), Baden-Baden, Germany, 5–9 June 2011; IEEE: Piscataway, NJ, USA, 2011; pp. 601–606. [CrossRef]
33. Bishop, C.M. Pattern Recognition and Feed-forward Networks. In *The MIT Encyclopedia of the Cognitive Sciences*; MIT Press: Cambridge, MA, USA, 1999; pp. 629–632.
34. Obaid, L.; Hamad, K.; Al-Ruzouq, R.; Dabous, S.A.; Ismail, K. Automating the Estimation of Turning Movement Rates at Multilane Roundabouts Using Unmanned Aerial Vehicles and Deep Learning. *Green Energy Intell. Transp.* **2025**, 100340. [CrossRef]
35. De Gelder, E.; Paardekooper, J.P.; Saberi, A.K.; Elrofai, H.; Den Camp, O.O.; Kraines, S.; Ploeg, J.; De Schutter, B. Towards an Ontology for Scenario Definition for the Assessment of Automated Vehicles: An Object-Oriented Framework. *IEEE Trans. Intell. Veh.* **2022**, *7*, 300–314. [CrossRef]

36. Schallau, T.; Naujokat, S.; Kullmann, F.; Howar, F. Tree-Based Scenario Classification: A Formal Framework for Coverage Analysis on Test Drives of Autonomous Vehicles. *arXiv* **2023**, arXiv:2307.05106. [CrossRef]
37. Müller, S. Theory and Applications of Runtime Monitoring Metric First-Order Temporal Logic. Doctoral Thesis, ETH Zurich, Zürich, Switzerland, 2009. [CrossRef]
38. Basin, D.; Klaedtke, F.; Müller, S.; Zălinescu, E. Monitoring Metric First-Order Temporal Properties. *J. ACM* **2015**, *62*, 1–45. [CrossRef]
39. Chen, H.; Ren, H.; Li, R.; Yang, G.; Ma, S. Generating Autonomous Driving Test Scenarios based on OpenSCENARIO. In Proceedings of the 2022 9th International Conference on Dependable Systems and Their Applications (DSA), Wulumuqi, China, 4–5 August 2022; IEEE: Piscataway, NJ, USA, 2022; pp. 650–658. [CrossRef]
40. Daoud, A.; Bunel, C.; Guériau, M. CornerSim: A Virtualization Framework to Generate Realistic Corner-Case Scenarios for Autonomous Driving Perception Testing. *Procedia Comput. Sci.* **2024**, *238*, 184–191. [CrossRef]
41. Klischat, M.; Althoff, M. Generating Critical Test Scenarios for Automated Vehicles with Evolutionary Algorithms. In Proceedings of the 2019 IEEE Intelligent Vehicles Symposium (IV), Paris, France, 9–12 June 2019; IEEE: Piscataway, NJ, USA, 2019; pp. 2352–2358.. [CrossRef]
42. Kim, J.; Kim, S.; Jeong, G.; Lee, E.; Lee, J. Rule-Based Translation from Natural Language to OpenSCENARIO by Injecting Various Disturbance for Driving Simulator. *IEEE Access* **2025**, *13*, 207200–207210. [CrossRef]
43. Laundal, K.M.; Richmond, A.D. Magnetic Coordinate Systems. *Space Sci. Rev.* **2017**, *206*, 27–59. [CrossRef]
44. Schlechtriemen, J.; Wedel, A.; Hillenbrand, J.; Breuel, G.; Kuhnert, K.-D. A Lane Change Detection Approach Using Feature Ranking with Maximized Predictive Power. In Proceedings of the 2014 IEEE Intelligent Vehicles Symposium Proceedings, Dearborn, MI, USA, 8–11 June 2014; IEEE: Piscataway, NJ, USA, 2014; pp. 108–114. [CrossRef]
45. Teo, T.-A.; Chang, M.-J.; Wen, T.-H. Automatic Vehicle Trajectory Behavior Classification Based on Unmanned Aerial Vehicle-Derived Trajectories Using Machine Learning Techniques. *ISPRS Int. J. Geo-Inf.* **2024**, *13*, 264. [CrossRef]
46. Xuan, Y.; Coifman, B. Lane Change Maneuver Detection from Probe Vehicle DGPS Data. In Proceedings of the 2006 IEEE Intelligent Transportation Systems Conference, Toronto, ON, Canada, 17–20 September 2006; IEEE: Piscataway, NJ, USA, 2006; pp. 624–629. [CrossRef]
47. Nagy, R.; Szalai, I. Vehicle Maneuver Recognition and Correction Algorithm for Road Quality Measurement System Optimization. *Meas. Sens.* **2025**, *38*, 101816. [CrossRef]
48. Akiba, T.; Sano, S.; Yanase, T.; Ohta, T.; Koyama, M. Optuna: A Next-generation Hyperparameter Optimization Framework. In Proceedings of the 25th ACM SIGKDD International Conference on Knowledge Discovery & Data Mining (KDD '19), Anchorage, AK, USA, 4–8 August 2019; pp. 2623–2631. [CrossRef]
49. Shekhar, S.; Bansode, A.; Salim, A. A Comparative study of Hyper-Parameter Optimization Tools. In Proceedings of the 2021 IEEE Asia-Pacific Conference on Computer Science and Data Engineering (CSDE), Brisbane, Australia, 8–10 December 2021; IEEE: Piscataway, NJ, USA, 2021; pp. 1–6. [CrossRef]
50. Wen, J.; Lyu, N.; Zheng, L. Exploring safety effects on urban expressway diverging areas: Crash risk estimation considering extreme conflict types. *Int. J. Inj. Control Saf. Promot.* **2024**, *32*, 25–39. [CrossRef] [PubMed]
51. Jia, Y.; Liu, Y.; Zhang, Y.; Chen, Z.; Lei, Z.; Zhang, Y. Lane changing enabled eco-driving control for plug-in hybrid electric vehicle under consecutive signalized intersection conditions. *Green Energy Intell. Transp.* **2026**, *5*, 100311. [CrossRef]
52. Dosovitskiy, A.; Ros, G.; Codevilla, F.; Lopez, A.; Koltun, V. CARLA: An open urban driving simulator. In Proceedings of the 1st Annual Conference on Robot Learning, Mountain View, CA, USA, 13–15 November 2017; Volume 78, pp. 1–16.